NASA/TP—2003-211890

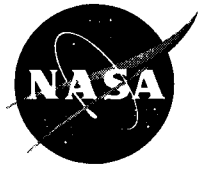

Novel Route to Transition Metal Isothiocyanate Complexes Using Metal Powders and Thiourea

Jerry D. Harris and William E. Eckles
Cleveland State University, Cleveland, Ohio

Aloysius F. Hepp
Glenn Research Center, Cleveland, Ohio

Stan A. Duraj and David G. Hehemann
Cleveland State University, Cleveland, Ohio

Phillip E. Fanwick
Purdue University, West Lafayette, Indiana

John Richardson
University of Louisville, Louisville, Kentucky

National Aeronautics and
Space Administration

Glenn Research Center

July 2003

Acknowledgments

We gratefully acknowledge the National Aeronautics and Space Administration for its support through grants NCC3–817, NCC3–869, and NAG3–2484, and through the NASA Glenn Research Center Director's Discretionary Fund.

Available from

NASA Center for Aerospace Information
7121 Standard Drive
Hanover, MD 21076

National Technical Information Service
5285 Port Royal Road
Springfield, VA 22100

Available electronically at http://gltrs.grc.nasa.gov

Novel Route to Transition Metal Isothiocyanate Complexes Using Metal Powders and Thiourea

Jerry D. Harris* and William E. Eckles
Cleveland State University
Cleveland, Ohio 44115

Aloysius F. Hepp
National Aeronautics and Space Administration
Glenn Research Center
Cleveland, Ohio 44135

Stan A. Duraj and David G. Hehemann
Cleveland State University
Cleveland, Ohio 44115

Phillip E. Fanwick
Purdue University
West Lafayette, Indiana 47907

John Richardson
University of Louisville
Louisville, Kentucky 40292

Summary

A new synthetic route to isothiocyanate-containing materials is presented. Eight isothiocyanate-4-methylpyridine (γ-picoline) compounds were prepared by refluxing metal powders (Mn, Fe, Co, Ni, and Cu) with thiourea in γ-picoline: compound 1—$(Hpic)_2[Mn(NCS)_4(pic)_2]\cdot 2pic$, compound 2—$(Hpic)_2[Fe(NCS)_4(pic)_2]\cdot 2pic$, compound 3—$[Fe(NCS)_2(pic)_4]\cdot pic$, compound 4—$[Co(NCS)_2(pic)_4]\cdot pic$, compound 6—$[Ni(NCS)_2(pic)_4]$, compound 7—$[Cu(NCS)_2(pic)_4]\cdot 2/3pic\cdot 1/3H_2O$, compound 8—$(Hpic)[Cu(NCS)_3(pic)_2]\cdot pic$, and compound 9—$[Cu(NCS)(pic)_2]_x$ (where pic = γ-picoline). Compound 5—$[Co(NCS)_2(pic)_4]$—was prepared by refluxing the metal powder with ammonium thiocyanate in γ-picoline. With the exception of compound 5, the isothiocyanate ligand was generated in situ by the isomerization of thiourea to $NH_4^+SCN^-$ at reflux temperatures. The complexes were characterized by x-ray crystallography. Compounds 1, 2, and 8 are the first isothiocyanate-4-methylpyridine anionic compounds ever prepared and structurally characterized. Compounds 1 and 2 are isostructural with four equatorially bound isothiocyanate ligands and two axially bound γ-picoline molecules. Compound 8 is a five-coordinate copper(II) molecule with a distorted square-pyramidal geometry. Coordinated picoline and two isothiocyanates form the basal plane and the remaining isothiocyanate is bound at the apex. Structural data are presented for all compounds.

*NASA Resident Research Associate at Glenn Research Center.

Background

Among the desirable attributes in any space-bound component, subsystem, or system are high specific power, high radiation tolerance, and high reliability, without sacrificing performance (ref. 1). The NASA Glenn Research Center is developing space-bound technologies in thin-film chalcopyrite solar cells and thin-film lithium (polymer) batteries (refs. 2 to 4). Metal chalcogenides (oxides, sulfides, selenides, and tellurides) are important materials for energy conversion ($CuInSe_2$, $CuInS_2$, CdTe, and ZnO) and storage devices (TiS_2, $LiCoO_2$, and SnO_2) (refs. 5 to 8). The key to achieving high specific power is the development of high-efficiency, thin-film materials that can be fabricated directly on flexible, lightweight, space-qualified durable substrates. Current thin-film cell fabrication approaches are limited by either (1) the ultimate efficiency that can be achieved with the device material and structure or (2) the requirement for high-temperature deposition processes that are incompatible with all presently known flexible polyimides or other suitable polymer substrate materials (ref. 1). There are two solutions for working around the second limitation: (1) develop new substrate (or superstrate) materials that are compatible with current deposition techniques, or (2) develop new deposition techniques that are compatible with existing materials (ref. 9). Glenn has chosen to focus on the latter approach.

Our objective is a chemically based approach to developing processes that will produce high-efficiency devices at temperatures below 400 °C (refs. 10 to 18). Such low temperatures minimize the problems associated with differences in the coefficients of thermal expansion between the substrate and thin-film devices and with decomposition of the substrate. Low-temperature processes also allow the devices to be prepared on metal-coated polymer substrates, such as Kapton (DuPont) or other suitable substrates, via a chemical spray process using advanced single-source precursors, or by direct electrochemical deposition (refs. 2 and 15). One novel approach is the use of single-source organometallic precursor molecules, which contain all the required chemically coordinated atoms. These molecules typically have low decomposition temperatures enabling the use of low-temperature substrates (refs. 12, 16, 17, and 19). In the course of our research effort, which focused on developing such precursors, we discovered an interesting chemical reaction that we report herein.

Introduction

Thiourea has been used as an industrial cleaning agent to remove scale buildup in boilers for many years. The scale is typically a mixture of metal oxides and metallic copper. The primary metal oxide is $FeFe_2O_4$, but oxides of nickel, zinc, and chromium are generally also present (ref. 20). In this application, thiourea is used in aqueous, acidic solutions. To explore the chemistry of thiourea in nonaqueous solution and to develop another potential route to material precursors, a series of reactions were performed, where thiourea and a metal powder were refluxed in 4-methylpyridine (γ-picoline) for extended periods of time.

During this study, nine isothiocyanate-4-methylpyridine complexes containing first-row transition metals between manganese and copper were prepared and structurally characterized. These include a series of five complexes of the type $[M(NCS)_2(pic)_4]$ (where M is Fe, Co, Ni, or Cu) and a bridging polymeric copper mono (isothiocyanate) compound, which have all been reported previously, along with manganese and iron N-bound tetrakis (isothiocyanate) compounds and a five-coordinate copper N-bound tris(isothiocyanate) compound. The latter three are the first anionic isothiocyanate-4-methylpyridine-metal complexes to be reported. We also report the discovery of a new method for producing isothiocyanate compounds that does not rely on a direct reaction with the thiocyanate ion. In this method, metal powders are reacted with thiourea in 4-methylpyridine to yield the isothiocyanate compounds. This differs from the more common methods of introducing the thiocyanate ligand into the coordination sphere of the metal by reacting soluble metal species with alkali metal thiocyanates, ammonium thiocyanate, or thiocyanogen in solution. The complexes that were prepared and characterized follow (where pic = γ-picoline):

(1) $(Hpic)_2[Mn(NCS)_4(pic)_2]\cdot 2pic$
(2) $(Hpic)_2[Fe(NCS)_4(pic)_2]\cdot 2pic$
(3) $[Fe(NCS)_2(pic)_4]\cdot pic$
(4) $[Co(NCS)_2(pic)_4]\cdot pic$
(5) $[Co(NCS)_2(pic)_4]$
(6) $[Ni(NCS)_2(pic)_4]$
(7) $[Cu(NCS)_2(pic)_4]\cdot 2/3pic\cdot 1/3H_2O$
(8) $(Hpic)[Cu(NCS)_3(pic)_2]\cdot pic$
(9) $[Cu(NCS)(pic)_2]_n$

Experimental Procedure

Techniques and Materials

Moisture- and air-sensitive materials were manipulated under an argon atmosphere employing standard Schlenk techniques and a double-manifold line. Solids were manipulated in an argon-filled glovebox. Solvents were freshly distilled from sodium benzophenone ketyl under N_2 prior to use. Metal powders (Strem Chemicals, Inc., Newburyport, MA), thiourea, and Celite (Aldrich Chemical Company, Milwaukee, WI) were used without further purification.

Synthesis of compound 1—$(Hpic)_2[Mn(NCS)_4(pic)_2]\cdot 2pic$.—Manganese powder (0.27 g, 4.9 mmol), thiourea (1.90 g, 25.0 mmol), and 4-methylpyridine (25 ml) were added to a round-bottom flask. After the solution was refluxed overnight, all the metal was consumed, yielding a red-brown solution. The solution was allowed to cool to room temperature and left undisturbed for approximately 4 weeks, during which time only a few small crystals appeared. The solution was then filtered through Celite and layered with hexanes. Large crystals grew within several days.

Synthesis of compound 2—$(H\text{-}pic)_2[Fe(NCS)_4(pic)_2]\cdot 2pic$.—Iron powder (0.28 g, 5.0 mmol), thiourea (1.90 g, 25.0 mmol), and 4-methylpyridine (25 ml) were added to a round-bottom flask. Upon refluxing, a yellow solution formed within a few hours and turned red after refluxing overnight. The solution refluxed for 4 days, and then was cooled and layered with 25 ml of hexanes. High-quality, dark red crystals grew in a few days.

Synthesis of compound 3—$[Fe(NCS)_2(pic)_4]\cdot pic$.—Iron powder (0.28 g, 5.0 mmol), thiourea (0.76 g, 10.0 mmol), and 4-methylpyridine (25 ml) were added to a Schlenk flask. Upon reflux, a yellow solution formed within a few hours. The solution remained unchanged after refluxing for 4 days but also contained an undetermined amount of unreacted iron. After cooling and setting undisturbed for 3 days, no crystals formed, but some product had precipitated. The solution was filtered through Celite, and the dark yellow filtrate was carefully layered with hexanes, which afforded diffraction-quality crystals after a few days.

Synthesis of compound 4—$[Co(NCS)_2(pic)_4]\cdot pic$.—Cobalt powder (0.59 g, 10.0 mmol), thiourea (1.52 g, 20.0 mmol), and 4-methylpyridine (25 ml) were added to a round-bottom flask. As the flask was heated and approached reflux temperature, the solution turned dark red. The solution was refluxed for 2 days, during which small crystals formed in the condenser. Heat was removed and the solution cooled to room temperature, forming many dark red crystals.

Synthesis of compound 5—$[Co(NCS)_2(pic)_4]$.—Cobalt powder (0.59 g, 10.0 mmol), ammonium thiocyanate (1.52 g, 20.0 mmol), and 4-methylpyridine (25 ml) were added to a round-bottom flask. As the flask was heated and approached reflux temperature, the solution turned bright blue. The solution was refluxed for 2 days and then allowed to cool to room temperature. After setting undisturbed for several days, the solution color changed to rose and several small crystals formed. The solution was filtered through Celite and layered with 25 ml of hexanes; in a few days, it yielded 5.0 g of blocky, rose-colored crystals.

Synthesis of compound 6—$[Ni(NCS)_2(pic)_4]$.—Nickel powder (0.59 g, 10.1 mmol), thiourea (1.52 g, 20.0 mmol), and 4-methylpyridine (25 ml) were added to a round-bottom flask. As the flask was heated and approached reflux temperature, the solution turned green. The solution was refluxed for 2 days, during which the solution turned brown and all the metal was consumed; small crystals formed at the bottom of the condenser. Upon cooling to room temperature, many large, dark green crystals formed.

Synthesis of compound 7—$[Cu(NCS)_2(pic)_4]\cdot 2/3pic\cdot 1/3H_2O$.—Copper powder (0.64 g, 10.1 mmol), thiourea (1.52 g, 25.0 mmol), and 4-methylpyridine (25 ml) were added to a Schlenk tube. The solution was warmed to 75 °C and held isothermal for 30 min while stirring. Heat was removed, and the dark solution was allowed to cool to room temperature. Colorless x-ray-diffraction-quality crystals formed in 3 days, along with a gray precipitate. While the colorless crystals were being manipulated, they were inadvertently exposed to air and changed to a green color.

Synthesis of compound 8—$(H\text{-}pic)[Cu(NCS)_3(pic)_2]\cdot pic$.—Copper powder (0.32 g, 5.0 mmol), thiourea (1.90 g, 25.0 mmol), and 4-methylpyridine (25 ml) were added to a round-bottom flask. After the solution refluxed for 2 days, all the metal powder was consumed. The orange solution was allowed to cool to room temperature, was filtered through Celite, and was layered with 30 ml of hexanes. X-ray-quality, yellow needle- and plate-shaped crystals grew in 3 days.

Synthesis of compound 9—$[Cu(NCS)(pic)_2]_n$.—Copper powder (0.64 g, 10.1 mmol), thiourea (1.52 g, 20.0 mmol), and 4-methylpyridine (25 ml) were added to a round-bottom flask. The solution refluxed for 3 days and was then cooled to room temperature; 0.05 g

(0.79 mmol) of metal remained unreacted. The yellow-orange solution was filtered through Celite and layered with 20 ml of hexanes. Many large yellow crystals grew in a few days.

X-Ray Structure Determinations

Single-crystal diffraction data were collected on an Enraf-Nonius (The Netherlands) CAD4 automated diffractometer with graphite monochromated MoKα radiation. Crystals were either mounted on glass fibers (compounds 1, 3 to 6, and 9) or sealed in capillaries (compounds 2, 7, and 8). Data were collected at either room temperature (compounds 1 to 6 and 8) or at –70 °C (compounds 7 and 9) using $\omega - 2\theta$ scans. Initial cell parameters were determined from least-squares refinements of 25 high-angle reflections obtained from an automatic centering program. Three check reflections were monitored periodically (every 83 to 150 min, depending on the data set) during the data collections to ensure crystal integrity during data collection. Check reflections for compound 1 revealed an intensity loss of 70.8 percent during data collection, so a linear decay correction was applied to the data set. No other data set showed any crystal degradation during data collection. All data sets were corrected for Lorentz and polarization effects, and with the exception of compounds 1, 4, and 6, an empirical absorption correction was applied to each data set by the use of DIFABS (ref. 21). Azimuthal scans of several reflections for compounds 1, 4, and 6 indicated that the crystals needed no absorption correction. Structures 1, 2, 5, and 7 to 9 were solved using SHELX–86 (ref. 22) and refined using MolEN (ref. 23); compounds 3, 4, and 6 were solved and refined using teXsan (ref. 24). The initial positions of heavy atoms in each structure were located by using the Patterson method, and the remaining atoms were located in successive least-squares refinements. All nonhydrogen atoms were refined anisotropically, with the exception of the disordered solvent molecules in compounds 3 and 4, which were refined isotropically. Hydrogen atoms were placed on the appropriate carbon atoms by using the standard riding model. Relevant crystallographic data are summarized in tables I to III, and atomic positional parameters are provided in tables IV to XII.

TABLE I.—CRYSTALLOGRAPHIC DATA FOR COMPOUNDS 1 AND 2

	Compound	
	1	2
Chemical name	$(Hpic)_2[Mn(NCS)_4(pic)_2]\cdot 2pic$	$(Hpic)_2[Fe(NCS)_4(pic)_2]\cdot 2pic$
Molecular formula	$MnC_{40}H_{44}N_{10}S_4$	$FeC_{40}H_{44}N_{10}S_4$
Formula weight	848.06	848.97
Temperature, K	293	293
Wavelength, Å	0.71073	0.71073
Space group	$P2_1/n$ (no. 14)	$P2_1/n$ (no. 14)
a, Å	12.691(3)	12.632(1)
b, Å	12.338(1)	12.335(2)
c, Å	14.478(4)	14.484(1)
α, deg	90	90
β, deg	90.44(2)	90.424(7)
γ, deg	90	90
V, Å^3	2266(1)	2256.8(7)
Z	2	2
Calculated density, g/cm^3	1.242	1.249
μ, cm^{-1}	4.94	5.48
Crystal size, mm	0.50 × 0.38 × 0.20	0.40 × 0.38 × 0.35
$2\theta_{max}$, deg	45	45
Scan method	ω – 2θ	ω – 2θ
Data (parameters)	3129 (254)	3114 (250)
Number observed, $I \geq 3\sigma(I)$	1849	1941
R	0.042	0.037
R_w	0.050	0.046
GOF	1.267	1.375
Maximum residual peak, eÅ^{-3}	0.54	0.36
CCDC number	175 214	175 215

TABLE II.—CRYSTALLOGRAPHIC DATA FOR COMPOUNDS 3, 4, 5, AND 6

	Compound			
	3	4	5	6
Chemical name	$[Fe(NCS)_2(pic)_4]\cdot pic$	$[Co(NCS)_2(pic)_4]\cdot pic$	$[Co(NCS)_2(pic)_4]$	$[Ni(NCS)_2(pic)_4]$
Molecular formula	$FeC_{27}H_{29}N_6S_2$	$CoC_{26}H_{28}N_6S_2$	$CoC_{26}H_{28}N_6S_2$	$NiC_{26}H_{28}N_6S_2$
Formula weight	557.53	547.60	547.61	547.37
Temperature, K	295	295	293	295
Wavelength, Å	0.71073	0.71073	0.71073	0.71073
Space group	$I4_1/a$ (no. 88)	$I4_1/a$ (no. 88)	$I4_1/a$ (no. 88)	$I4_1/a$ (no. 88)
a, Å	17.030(4)	16.839(2)	16.644(4)	16.635(4)
b, Å	17.030(4)	16.839(2)	16.644(4)	16.635(4)
c, Å	23.377(4)	22.820(3)	22.848(2)	22.673(8)
α, deg	90	90	90	90
β, deg	90	90	90	90
γ, deg	90	90	90	90
V, Å^3	6787(1)	6470(1)	6329	6269(2)
Z	8	8	8	8
Calculated density, g/cm^3	1.091	1.124	1.149	1.16
μ, cm^{-1}	5.89	6.81	6.88	7.74
Crystal size, mm	$0.04 \times 0.05 \times 0.05$	$0.42 \times 0.37 \times 0.51$	$0.49 \times 0.38 \times 0.25$	$0.40 \times 0.50 \times 0.20$
$2\theta_{max}$, deg	50	50	45	50
Scan method	$\omega - 2\theta$	$\omega - 2\theta$	$\omega - 2\theta$	$\omega - 2\theta$
Data (parameters)	3063 (171)	2935 (167)	2308 (159)	2822 (159)
Number observed, $I \geq 3\sigma(I)$	1776	1893	1568	1936
R	0.072	0.050	0.037	0.045
R_w	0.096	0.060	0.047	0.057
GOF	4.33	3.43	1.261	1.62
Maximum residual peak, eÅ^{-3}	0.53	0.39	0.28	0.46
CCDC number	175 217	175 218	186 429	175 219

TABLE III.—CRYSTALLOGRAPHIC DATA FOR COMPOUNDS 7, 8, AND 9

	Compound		
	7	8	9
Chemical name	$[Cu(NCS)_2(pic)_4]\cdot 2/3pic\cdot 1/3H_2O$	$(Hpic)[Cu(NCS)_3(pic)_2]\cdot pic$	$[Cu(NCS)(pic)_2]_n$
Molecular formula	$CuC_{30}H_{33.33}N_{6.67}O_{0.33}S_2$	$CuC_{27}H_{29}N_7S_3$	$CuC_{13}H_{14}N_3S$
Formula weight	620.31	611.31	307.88
Temperature, K	203	293	203
Wavelength, Å	0.71073	0.71073	0.71073
Space group	$R\bar{3}$ (no. 148)	*Cc* (no. 9)	$P2_1$ (no. 4)
a, Å	16.070(1)	14.656(1)	8.4138(8)
b, Å	16.070(1)	15.635(2)	5.8127(7)
c, Å	16.070(1)	14.390(1)	14.459(2)
α, deg	114.714(5)	90	90
β, deg	114.714(5)	112.886(7)	106.783(9)
γ, deg	114.714(5)	90	90
V, Å^3	2381(2)	3038(1)	677.0(3)
Z	3	4	2
Calculated density, g/cm^3	1.297	1.337	1.510
μ, cm^{-1}	8.29	9.45	17.49
Crystal size, mm	$0.56 \times 0.50 \times 0.39$	$0.46 \times 0.44 \times 0.22$	$0.47 \times 0.47 \times 0.38$
$2\theta_{max}$, deg	50	46	55
Scan method	$\omega - 2\theta$	$\omega - 2\theta$	$\omega - 2\theta$
Data (parameters)	2982 (175)	2201 (341)	1590 (162)
Number observed, $I \geq 3\sigma(I)$	2362	1734	1524
R	0.071	0.043	0.028
R_w	0.090	0.053	0.037
GOF	2.884	1.657	1.501
Maximum residual peak, eÅ^{-3}	2.98	0.46	0.36
CCDC number	186 430	175 216	175 220

TABLE IV.—ATOMIC COORDINATES AND ISOTROPIC DISPLACEMENT COEFFICIENTS (B) FOR COMPOUND 1 ($(Hpic)_2[Mn(NCS)_4(pic)_2]\cdot pic$)

Atom	x	y	z	[a]B, Å^2
Mn	0.5	0.0	0.5	4.40(2)
S1	.3655(1)	.3769(1)	.4824(1)	6.01(3)
S2	.1262(1)	−.1170(1)	.5210(1)	6.58(3)
N1	.4517(3)	.1699(3)	.4744(3)	5.9(1)
N2	.3315(3)	−.0431(3)	.5036(3)	5.6(1)
N11	.4993(2)	.0362(3)	.6562(3)	4.83(8)
N101	.5710(2)	.4041(3)	.2394(3)	4.90(9)
N201	.4400(2)	.5713(3)	.2517(3)	4.79(9)
C1	.4165(3)	.2553(4)	.4782(3)	4.5(1)
C2	.2465(3)	−.0728(3)	.5104(3)	4.3(1)
C12	.4408(3)	.1140(4)	.6955(3)	5.3(1)
C13	.4499(4)	.1438(4)	.7862(3)	5.7(1)
C14	.5216(4)	.0956(4)	.8430(3)	5.4(1)
C15	.5806(4)	.0148(4)	.8039(3)	7.2(1)
C16	.5672(4)	−.0110(4)	.7134(3)	6.7(1)
C17	.5375(5)	.1286(4)	.9419(4)	8.0(2)
C102	.5922(4)	.3496(4)	.3156(3)	6.3(1)
C103	.6473(4)	.2539(4)	.3142(3)	6.4(1)
C104	.6821(3)	.2128(3)	.2322(3)	4.7(1)
C105	.6620(4)	.2709(4)	.1536(3)	5.6(1)
C106	.6054(4)	.3661(4)	.1608(3)	6.0(1)
C107	.7432(4)	.1086(4)	.2288(4)	7.1(1)
C202	.3817(3)	.5971(3)	.1781(3)	4.7(1)
C203	.3036(3)	.6726(3)	.1833(3)	4.6(1)
C204	.2822(3)	.7233(3)	.2655(3)	4.6(1)
C205	.3433(4)	.6968(4)	.3401(3)	5.6(1)
C206	.4218(4)	.6199(4)	.3308(3)	5.6(1)
C207	.1954(4)	.8044(5)	.2729(4)	7.8(2)
H1	.502(4)	.499(4)	.250(4)	[b]12(2)

[a]$B = (4/3)[a^2\beta(1,1) + b^2\beta(2,2) + c^2\beta(3,3) + ab(\cos\gamma)\,\beta(1,2) + ac(\cos\beta)\,\beta(1,3) + bc(\cos\alpha)\,\beta(2,3)]$.

[b]Atom was refined isotropically.

TABLE V.—ATOMIC COORDINATES AND ISOTROPIC DISPLACEMENT COEFFICIENTS (B) FOR COMPOUND 2 ($(Hpic)_2[Fe(NCS)_4(pic)_2]\cdot 2pic$)

Atom	x	y	z	[a]B, Å^2
Fe	0.5	0.0	0.5	4.42(2)
S1	.63232(9)	.37297(9)	.52022(8)	5.98(3)
S2	.12932(8)	.1152(1)	.52234(8)	6.53(3)
N1	.5463(2)	.1655(3)	.5260(2)	5.38(8)
N2	.3364(2)	.0419(3)	.5048(2)	5.32(8)
N31	.5004(2)	.0376(2)	.3485(2)	4.81(7)
C1	.5818(3)	.2518(3)	.5233(2)	4.36(8)
C2	.2505(3)	.0718(3)	.5118(2)	4.19(8)
C32	.5608(3)	.1128(3)	.3100(3)	5.3(1)
C33	.5531(3)	.1430(3)	.2187(3)	5.9(1)
C34	.4803(3)	.0951(3)	.1618(3)	5.7(1)
C35	.4195(4)	.0160(4)	.2006(3)	7.3(1)
C36	.4317(3)	−.0102(4)	.2918(3)	6.8(1)
C37	.4662(4)	.1282(4)	.0622(3)	8.2(1)
N101	.9422(2)	.0690(2)	.7512(2)	4.95(7)
N201	1.0704(2)	−.0980(2)	.7373(2)	5.15(7)
C102	.8824(3)	.0970(3)	.6782(3)	4.94(9)
C103	.8043(3)	.1720(3)	.6838(2)	4.80(9)
C104	.7828(3)	.2225(3)	.7663(3)	4.75(9)
C105	.8456(3)	.1931(3)	.8405(3)	5.7(1)
C106	.9232(3)	.1177(3)	.8305(3)	5.7(1)
C107	.6959(4)	.3039(4)	.7750(3)	7.8(1)
C202	1.0923(3)	−.1539(4)	.8124(3)	6.6(1)
C203	1.1470(3)	−.2498(4)	.8106(3)	6.7(1)
C204	1.1828(3)	−.2908(3)	.7290(3)	4.77(9)
C205	1.1607(3)	−.2314(3)	.6515(3)	5.8(1)
C206	1.1052(3)	−.1365(3)	.6580(3)	6.2(1)
C207	1.2435(4)	−.3942(4)	.7255(3)	7.1(1)

[a]$B = (4/3)[a^2\beta(1,1) + b^2\beta(2,2) + c^2\beta(3,3) + ab(\cos\gamma)\,\beta(1,2) + ac(\cos\beta)\,\beta(1,3) + bc(\cos\alpha)\,\beta(2,3)]$.

TABLE VI.—ATOMIC COORDINATES AND ISOTROPIC DISPLACEMENT COEFFICIENTS (*B*) FOR COMPOUND 3 ($Fe(NCS)_2(pic)_4$)

Atom	*x*	*y*	*z*	$^aB_{eq}$
Fe1	0.000	0.250	–0.19392(7)	4.47(4)
S1	.1267(2)	–.0020(1)	–.1960(1)	8.70(9)
N1	.0747(4)	.1517(4)	–.1959(3)	5.9(2)
N2	.0720(4)	.3078(3)	–.2616(3)	4.5(2)
N3	–.0751(4)	.1975(4)	–.1267(3)	5.4(2)
C1	.0968(4)	.0880(5)	–.1960(4)	5.0(2)
C2	.1511(5)	.3070(5)	–.2623(4)	5.0(2)
C3	.1949(5)	.3431(5)	–.3035(4)	5.6(2)
C4	.1592(5)	.3824(5)	–.3486(4)	5.4(2)
C5	.0790(5)	.3839(5)	–.3486(4)	5.4(2)
C6	.0381(4)	.3461(5)	–.3046(4)	5.4(2)
C7	.2034(6)	.4210(6)	–.3949(4)	8.6(3)
C8	–.1079(6)	.2426(6)	–.0877(5)	7.6(3)
C9	–.1517(7)	.2116(8)	–.0425(5)	8.9(4)
C10	–.1617(6)	.1306(8)	–.0388(5)	8.3(4)
C11	–.1285(7)	.0868(6)	–.0786(5)	9.2(4)
C12	–.0889(6)	.1209(5)	–.1212(4)	6.7(3)
C13	–.2095(7)	.1025(8)	.0133(5)	11.8(4)
C15	.289(1)	.199(2)	.226(1)	6.991
C16	.294(1)	.244(2)	.275(1)	7.620
C17	.235(2)	.297(2)	.289(1)	6.212
C18	.170(1)	.305(1)	.252(1)	6.685
C19	.165(1)	.260(2)	.203(1)	7.223
C20	.225(2)	.207(2)	.189(1)	7.246

$^aB_{eq} = (8/3)\pi^2(U_{11}(aa)^2 + U_{22}(bb)^2 + U_{33}(cc)^2 + 2U_{12}aa\ bb \cos\gamma + 2U_{13}aa\ cc \cos\beta + 2U_{23}bb\ cc \cos\alpha)$.

TABLE VII.—ATOMIC COORDINATES AND ISOTROPIC DISPLACEMENT COEFFICIENTS (*B*) FOR COMPOUND 4 ($Co(NCS)_2(pic)_4$)

Atom	*x*	*y*	*z*	$^aB_{eq}$
Co	0.00	0.25	–0.06064(4)	4.19(2)
S1	.25352(10)	.1286(1)	–.05755(9)	8.47(6)
N1	.0953(3)	.1703(2)	–.0585(2)	5.1(1)
N2	.0607(2)	.3187(2)	.0072(2)	4.2(1)
N3	–.0579(3)	.1799(2)	–.1286(2)	5.0(1)
C1	.1607(4)	.1529(3)	–.0578(2)	4.7(1)
C2	.0623(3)	.3981(3)	.0079(2)	4.5(1)
C3	.0996(3)	.4415(3)	.0509(2)	5.2(1)
C4	.1383(3)	.4036(3)	.0963(2)	5.0(1)
C5	.1374(3)	.3232(3)	.0951(2)	5.2(1)
C6	.0996(3)	.2823(3)	.0512(2)	4.9(1)
C7	.1782(4)	.4485(4)	.1445(3)	7.9(2)
C8	–.0148(4)	.1416(4)	–.1683(3)	6.6(2)
C9	–.0477(5)	.0995(4)	–.2148(3)	7.5(2)
C10	–.1278(5)	.0968(4)	–.2207(3)	7.1(2)
C11	–.1718(4)	.1344(4)	–.1792(3)	7.5(2)
C12	–.1352(4)	.1756(4)	–.1347(3)	6.4(2)
C13	–.1657(5)	.0512(5)	–.2711(3)	11.7(3)
C14	.011(6)	.210(3)	–.400(2)	19(2)
C15	–.019(3)	.164(3)	–.396(2)	14(1)

$^aB_{eq} = (8/3)\pi^2(U_{11}(aa)^2 + U_{22}(bb)^2 + U_{33}(cc)^2 + 2U_{12}aa\ bb \cos\gamma + 2U_{13}aa\ cc \cos\beta + 2U_{23}bb\ cc \cos\alpha)$.

TABLE VIII.—ATOMIC COORDINATES AND ISOTROPIC DISPLACEMENT COEFFICIENTS (*B*) FOR COMPOUND 5 ($Co(NCS)_2(pic)_4$)

Atom	*x*	*y*	*z*	[a]*B*, Å^2
Co	0.0	0.75	0.06072(3)	3.91(1)
S	.25702(7)	.63050(8)	.05841(7)	7.75(3)
N	.0954(2)	.6688(2)	.0591(1)	4.87(7)
N11	−.0585(2)	.6806(2)	.1287(1)	4.62(7)
N21	.0619(2)	.8178(2)	−.0067(1)	4.02(6)
C	.1625(2)	.6526(2)	.0586(2)	4.45(8)
C12	−.1373(3)	.6761(3)	.1350(2)	5.9(1)
C13	−.1746(3)	.6383(3)	.1808(2)	7.1(1)
C14	−.1304(3)	.6014(3)	.2231(2)	6.8(1)
C15	−.0495(3)	.6043(3)	.2169(2)	7.1(1)
C16	−.0157(3)	.6437(3)	.1699(2)	6.2(1)
C17	−.1672(4)	.5590(4)	.2750(2)	10.6(2)
C22	.0634(2)	.8983(2)	−.0077(2)	4.43(8)
C23	.1012(2)	.9416(2)	−.0505(2)	4.85(9)
C24	.1398(2)	.9031(2)	−.0959(2)	4.75(9)
C25	.1383(2)	.8214(2)	−.0949(2)	5.05(9)
C26	.0998(2)	.7815(2)	−.0506(2)	4.77(9)
C27	.1797(3)	.9489(3)	−.1441(2)	7.6(1)

[a]$B = (4/3)[a^2\beta(1,1) + b^2\beta(2,2) + c^2\beta(3,3) + ab(\cos\gamma)\,\beta(1,2) + ac(\cos\beta)\,\beta(1,3) + bc(\cos\alpha)\,\beta(2,3)]$.

TABLE IX.—ATOMIC COORDINATES AND ISOTROPIC DISPLACEMENT COEFFICIENTS (*B*) FOR COMPOUND 6 ($Ni(NCS)_2(pic)_4$)

Atom	*x*	*y*	*z*	[a]B_{eq}
Ni	0.000	−0.250	0.06136(3)	3.35(2)
S	−.25643(7)	−.36987(8)	.05802(6)	6.94(4)
N1	−.0944(2)	−.3313(2)	.0599(1)	4.18(8)
N2	.0608(2)	−.3168(2)	−.0052(1)	3.48(7)
N3	−.0580(2)	−.1818(2)	.1286(1)	4.02(7)
C1	−.1614(2)	−.3475(2)	.0591(2)	3.91(9)
C2	.0629(2)	−.3971(2)	−.0055(2)	3.85(8)
C3	.1011(2)	−.4407(2)	−.0487(2)	4.40(9)
C4	.1397(2)	−.4022(2)	−.0945(2)	4.14(9)
C5	.1379(2)	−.3194(2)	−.0940(2)	4.32(9)
C6	.0991(2)	−.2799(2)	−.0497(1)	4.25(9)
C7	.1806(3)	−.4476(3)	−.1433(2)	6.9(1)
C8	−.0145(3)	−.1454(3)	.1704(2)	5.3(1)
C9	−.0484(3)	−.1060(3)	.2176(2)	6.1(1)
C10	−.1304(3)	−.1026(3)	.2234(2)	6.0(1)
C11	−.1754(3)	−.1378(3)	.1797(2)	6.1(1)
C12	−.1373(2)	−.1769(2)	.1337(2)	4.88(10)
C13	−.1691(4)	−.0616(4)	.2753(2)	9.4(2)

[a]$B_{eq} = (8/3)\pi^2(U_{11}(aa)^2 + U_{22}(bb)^2 + U_{33}(cc)^2 + 2U_{12}aa\,bb\cos\gamma + 2U_{13}aa\,cc\cos\beta + 2U_{23}bb\,cc\cos\alpha$.

TABLE X.—ATOMIC COORDINATES AND ISOTROPIC DISPLACEMENT COEFFICIENTS (*B*) FOR COMPOUND 7 ($[Cu(NCS)_2(pic)_4]\cdot 2/3pic\cdot 1/3H_2O$)

Atom	*x*	*y*	*z*	[a]*B*, Å^2
Cu	0.0	0.5	0.0	3.01(2)
S1	.2448(1)	.9459(1)	.2991(1)	6.46(5)
N1	.0939(3)	.6840(2)	.0945(3)	3.5(1)
N21	.1156(2)	.5174(2)	−.0304(2)	2.90(9)
N31	.1613(2)	.5765(3)	.2097(2)	3.4(1)
C1	.1560(3)	.7935(3)	.1783(3)	3.1(1)
C22	.1549(3)	.4601(3)	−.0277(3)	3.3(1)
C23	.2274(3)	.4647(3)	−.0537(3)	3.7(1)
C24	.2632(3)	.5332(3)	−.0836(3)	3.7(1)
C25	.2256(3)	.5954(3)	−.0831(3)	3.7(1)
C26	.1520(3)	.5859(3)	−.0573(3)	3.5(1)
C27	.3403(4)	.5390(4)	−.1145(4)	6.3(2)
C32	.1466(3)	.4989(3)	.2267(3)	3.6(1)
C33	.2392(3)	.5443(3)	.3438(3)	3.8(1)
C34	.3553(3)	.6770(3)	.4517(3)	3.8(1)
C35	.3724(4)	.7584(3)	.4351(3)	4.0(1)
C36	.2730(4)	.7037(3)	.3141(3)	4.0(1)
C37	.4607(4)	.7327(4)	.5816(4)	5.5(2)
O300	.5	.5	.5	[b]16.4(8)
N101	.241(2)	.241	.241	[b]15.1(6)
C102	.172(1)	.242(1)	.142(1)	[b]13.0(6)
C103	.058(2)	.178(2)	.022(2)	[b]18.0(9)
C104	−.067(2)	.021(2)	−.0112(2)	[b]19(1)

[a]$B = (4/3)[a^2\beta(1,1) + b^2\beta(2,2) + c^2\beta(3,3) + ab(\cos\gamma)\,\beta(1,2) + ac(\cos\beta)\,\beta(1,3) + bc(\cos\alpha)\,\beta(2,3)]$.

[b]Atom was refined isotropically.

TABLE XI.—ATOMIC COORDINATES AND ISOTROPIC DISPLACEMENT COEFFICIENTS (B) FOR COMPOUND 8 ((Hpic)[Cu(NCS)$_3$(pic)$_2$]·pic)

Atom	x	y	z	[a]B, Å^2
Cu	0.97940	0.75845(5)	0.17890	4.48(2)
S1	.7094(2)	.7093(2)	.2681(2)	9.57(7)
S2	1.2084(2)	.8210(2)	.0327(2)	8.43(6)
S7	1.3046(2)	.7230(2)	.4406(3)	8.08(8)
Nl	.8706(5)	.7326(4)	.2179(5)	5.3(2)
N2	1.0633(5)	.7883(5)	.1051(5)	5.8(2)
N7	1.1045(6)	.7426(5)	.3284(6)	7.2(2)
N31	.9641(4)	.8865(4)	.1997(4)	4.5(1)
N41	.9852(4)	.6341(4)	.1390(4)	4.3(1)
Cl	.8026(6)	.7228(5)	.2385(6)	4.9(2)
C2	1.1257(5)	.8017(5)	.0776(6)	4.7(2)
C7	1.1892(6)	.7346(5)	.3754(6)	4.6(2)
C32	1.0415(5)	.9361(5)	.2349(6)	5.0(2)
C33	1.0374(7)	1.0214(5)	.2512(7)	5.7(2)
C34	.9487(6)	1.0607(5)	.2296(6)	5.3(2)
C35	.8660(6)	1.0091(5)	.1888(7)	5.7(2)
C36	.8755(5)	.9230(5)	.1744(6)	5.2(2)
C37	.9421(8)	1.1535(6)	.2472(8)	8.1(3)
C42	.9020(5)	.5866(5)	.0988(6)	5.0(2)
C43	.9038(6)	.5015(5)	.0774(6)	5.4(2)
C44	.9923(6)	.4601(5)	.1020(6)	5.7(2)
C45	1.0755(6)	.5083(6)	.1396(6)	5.8(2)
C46	1.0704(5)	.5938(5)	.1575(6)	5.4(2)
C47	.9970(8)	.3654(6)	.0826(9)	8.8(3)
N51	−.1744(5)	.9289(5)	.4400(5)	5.7(2)
N61	.6317(5)	.9418(5)	.4027(5)	5.6(2)
C52	−.1285(7)	.8562(6)	.4489(8)	7.0(3)
C53	−.0272(7)	.8524(6)	.4739(7)	6.8(3)
C54	.0258(6)	.9263(5)	.4888(6)	4.9(2)
C55	−.0250(6)	1.0012(5)	.4750(6)	5.4(2)
C56	−.1239(7)	1.0012(6)	.4521(7)	6.0(2)
C57	.1354(7)	.9251(7)	.5157(8)	7.4(3)
C62	.5869(6)	1.0177(6)	.3837(6)	5.6(2)
C63	.4872(6)	1.0268(5)	.3539(6)	5.8(2)
C64	.4281(6)	.9555(6)	.3413(6)	5.8(2)
C65	.4746(6)	.8773(6)	.3612(8)	6.8(3)
C66	.5754(6)	.8728(6)	.3924(7)	6.1(2)
C67	.3181(7)	.9602(9)	.3044(8)	8.7(3)

[a]$B = (4/3)[a^2\beta(1,1) + b^2\beta(2,2) + c^2\beta(3,3) + ab(\cos\gamma)\,\beta(1,2) + ac(\cos\beta)\,\beta(1,3) + bc(\cos\alpha)\,\beta(2,3)]$.

TABLE XII.—ATOMIC COORDINATES AND ISOTROPIC DISPLACEMENT COEFFICIENTS (B) FOR COMPOUND 9 ([Cu(NCS)(pic)$_2$]$_n$)

Atom	x	y	z	[a]B, Å^2
Cu	0.49418(4)	0.55550	0.22090(2)	2.692(6)
S1	.72317(8)	.8072(2)	.26555(5)	2.82(1)
Nl	.5643(3)	.2355(5)	.2369(2)	2.97(5)
N21	.3651(3)	.6270(5)	.0847(2)	2.50(4)
N31	.3489(3)	.6439(5)	.3194(2)	2.56(4)
Cl	.6272(3)	1.0563(6)	.2488(2)	2.33(4)
C22	.3749(3)	.4916(5)	.3960(2)	2.78(6)
C23	.3048(3)	.5438(7)	.4683(2)	2.81(5)
C24	.2178(3)	.7479(6)	.4641(2)	2.44(5)
C25	.2070(4)	.8889(6)	.3858(2)	3.14(6)
C26	.2808(3)	.8255(7)	.3163(2)	3.17(6)
C27	.1370(4)	.8125(8)	.5407(2)	3.49(6)
C32	.3695(4)	.8386(6)	.0403(2)	2.99(6)
C33	.2678(4)	.9026(6)	−.0496(2)	2.86(6)
C34	.1384(3)	.7600(6)	−.0976(2)	2.56(5)
C35	.1188(3)	.5584(8)	−.0528(2)	3.36(6)
C36	.2239(4)	.5059(6)	.0375(2)	3.10(6)
C37	.0295(4)	.8250(8)	−.1960(2)	3.58(7)

[a]$B = (4/3)[a^2\beta(1,1) + b^2\beta(2,2) + c^2\beta(3,3) + ab(\cos\gamma)\,\beta(1,2) + ac(\cos\beta)\,\beta(1,3) + bc(\cos\alpha)\,\beta(2,3)]$.

Results and Discussion

As expected, the composition of the isolated products depends on the stoichiometry of the metal powders and thiourea. If modest molar ratios of 1:2 (metal:thiourea) are used, then the previously reported materials (compounds 3, 4, 6, 7, and 9) are obtained. However, if a large excess of thiourea is added (a metal to thiourea ratio of 1:5), then the anionic compounds (compounds 1, 2, and 8) are produced. The latter three are the first anionic isothiocyanate-4-methylpyridine-metal complexes to be reported.

Isostructural compounds 1 and 2 consist of six-coordinate metal centers with four equatorially bound isothiocyanate ligands and two axially bound 4-methylpyridine molecules to give an octahedral geometry. The unit cell for each compound also contains two protonated 4-methylpyridine molecules as counterions and two entrained solvent molecules. The products are shown in figures 1 and 2. Axially bound picoline molecules are coplanar, consistent with an inversion center being located at the metal atom sites. In the solid, the metal and the four isothiocyanate ligands form sheets parallel to the a–b plane, located at $z = 0$ and 1/2. The picoline rings extend above and below the metal-isothiocyanate layers. The rings of the bound picoline interleave with the rings of the entrained solvent and counterion molecules to yield efficient packing in the solid. In the manganese compound (1), Mn–N distances were found to be 2.05(4) Å and 2.214(4) Å for the bound isothiocyanate and 2.306(4) Å for the coordinated solvent (table XIII). In the iron compound (2), corresponding Fe–N distances measure 2.132(3) Å and 2.155(4) Å for the bound isothiocyanate and 2.243(3) Å for the coordinated 4-methylpyridine (table XIV). The isothiocyanate ligands in both compounds are nearly linear, with N=C=S bond angles ranging from 179.0(4)° to 179.3(5)° in the Mn compound and 179.4(3)° to 179.5(3)° in the Fe compound. Metal–N=S angles range from 165.9(4)° to 174.1(4)° for compound 1 and from 166.2(3)° to 174.3(3)° for compound 2. All bond distances and angles in these compounds are consistent with the similar Mn^{2+} and Fe^{2+} neutral compounds of $[Mn(NCS)_2(4\text{-}MePy)_4]$ and $[Fe(NCS)_2(4\text{-}MePy)_4]$ (refs. 25 to 27).

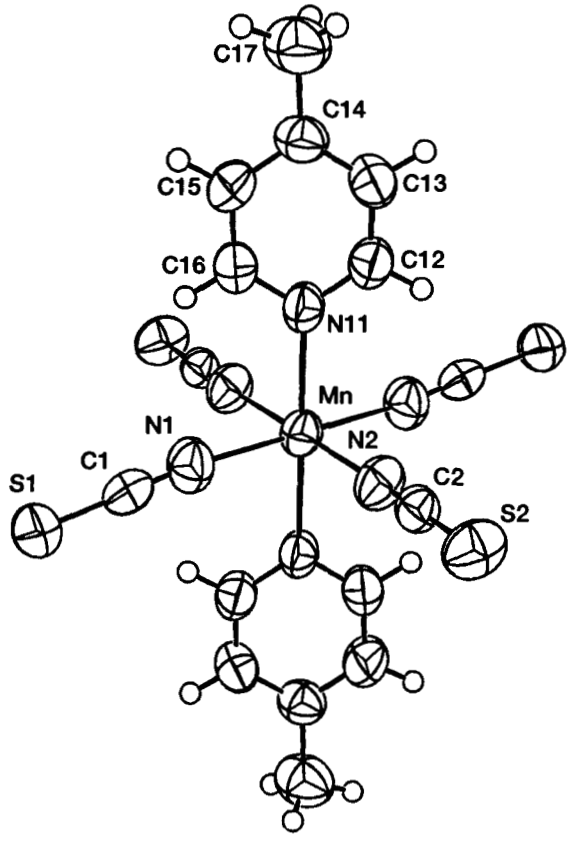

Figure 1.—ORTEP diagram of compound 1 ($[Mn(NCS)_4(pic)_2]^{2-}$) with hydrogens. Atoms are represented by ellipsoids at 50-percent probability.

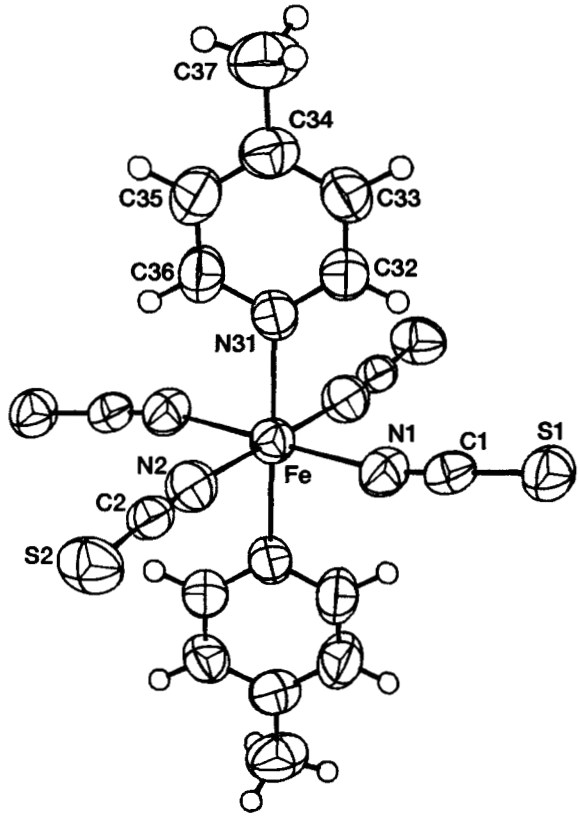

Figure 2.—ORTEP diagram of compound 2 ($[Fe(NCS)_4(pic)_2]^{2-}$) with hydrogens. Atoms are represented by ellipsoids at 50-percent probability.

TABLE XIII.—SELECTED BOND LENGTHS AND BOND ANGLES WITH ESTIMATED STANDARD DEVIATIONS (NUMBERS IN PARENTHESES) FOR COMPOUND 1 ($(Hpic)_2[Mn(NCS)_4(pic)_2]\cdot 2pic$)

Bond	Bond length, Å	Bond	Bond angle, deg
Mn–N1	2.214(4)	Mn–N1–C1	165.9(4)
Mn–N2	2.205(4)	Mn–N2–C2	174.1(4)
Mn–N11	2.306(4)	N1–C1–S1	179.3(5)
N1–C1	1.146(5)	N2–C2–S2	179.0(4)
N2–C2	1.145(5)	N1–Mn–N2	88.0(1)
C1–S1	1.636(6)	N1–Mn–N11	88.7(1)
C2–S2	1.628(5)	N2–Mn–N11	90.7(1)

TABLE XIV.—SELECTED BOND LENGTHS AND BOND ANGLES WITH ESTIMATED STANDARD DEVIATIONS (NUMBERS IN PARENTHESES) FOR COMPOUND 2 ($(Hpic)_2[Fe(NCS)_4(pic)_2]\cdot 2pic$)

Bond	Bond length, Å	Bond	Bond angle, deg
Fe–N1	2.155(4)	Fe–N1–C1	166.2(3)
Fe–N2	2.132(3)	Fe–N2–C2	174.3(3)
Fe–N31	2.243(3)	N1–C1–S1	179.5(3)
N1–C1	1.157(5)	N2–C2–S2	179.4(3)
N2–C2	1.151(4)	N1–Fe–N2	91.5(1)
C1–S1	1.625(5)	N1–Mn–N31	88.4(1)
C2–S2	1.630(4)	N2–Mn–N31	89.5(1)

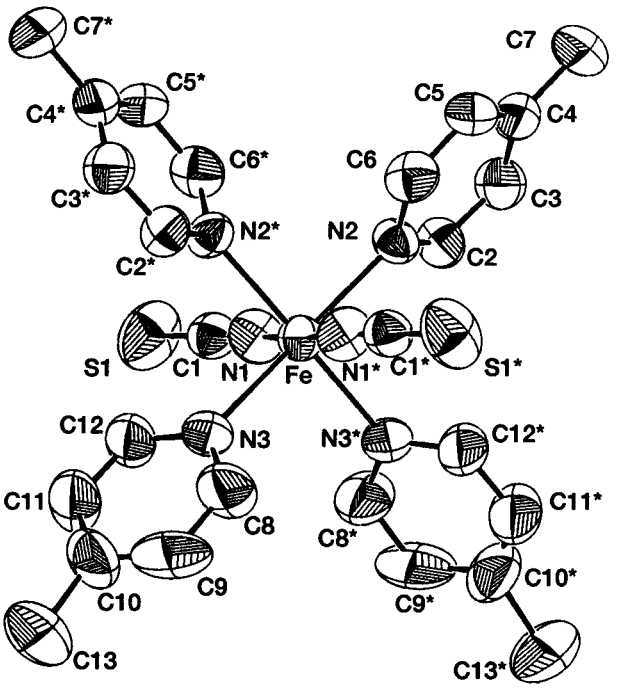

Figure 3.—ORTEP diagram of compound 3 ($Fe(NCS)_2(pic)_4$) without hydrogens. Atoms are represented by ellipsoids at 50-percent probability. An asterisk indicates an equivalent atom that is related by symmetry.

Isostructural compounds 3, 4, and 6 consist of divalent metals coordinated to four γ-picoline molecules and two isothiocyanate groups that give them a classic "propeller" shape. The products are shown in figures 3, 4, and 5. These materials, along with compounds 5 and 7, are members of a class of materials of the type MP_4X_2 (where M is a divalent transition metal, P is a pyridine derivative, and X is a halide or pseudohalide), which form clathrates with many guest molecules (ref. 28). Several members of this family have been extensively studied ($[Ni(NCS)_2(pic)_4]$ in particular) because of their ability to host a wide range of guest molecules in channels in their extended networks (refs. 29 to 31). Some structures exhibit zeolitic properties and permit guest-desorption without lattice destruction (ref. 32).

Both the Fe- and Co-containing structures (compounds 3 and 4) contained an occluded solvent molecule, but in each case the γ-picoline was extremely disordered. In the Fe case, a ring could be formed across a site with $\bar{4}$ symmetry. The solvent was modeled with a benzene ring at 25-percent occupancy. Neither the 4-methyl group nor the nitrogen could be identified because of either overlapping of groups in the disordered area or spinning of the

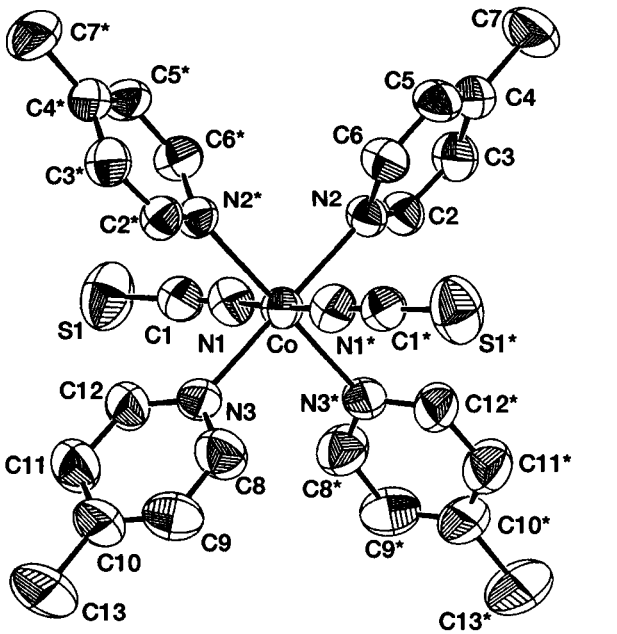

Figure 4.—ORTEP diagram of compound 4 ($Co(NCS)_2(pic)_4$) without hydrogens. Atoms are represented by ellipsoids at 50-percent probability. An asterisk indicates an equivalent atom that is related by symmetry.

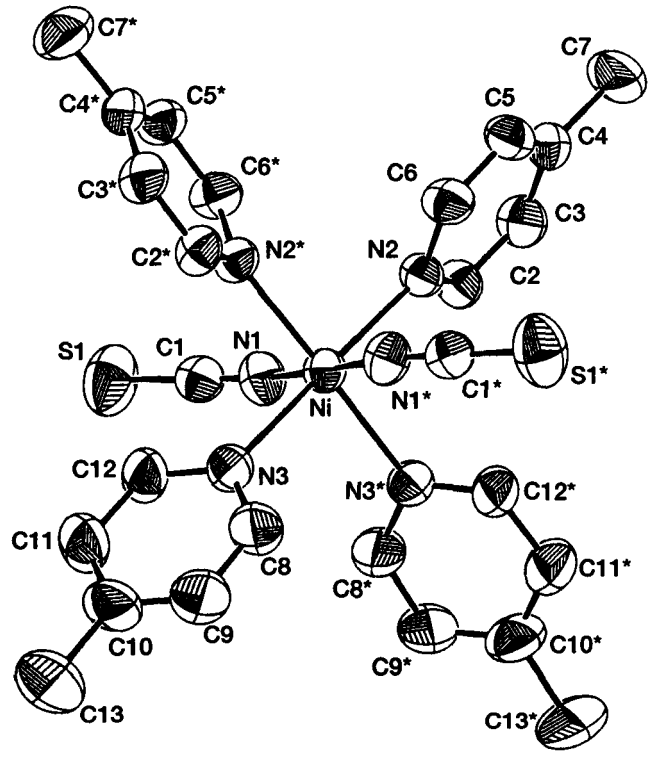

Figure 5.—ORTEP diagram of compound 6 ($Ni(NCS)_2(pic)_4$) without hydrogens. Atoms are represented by ellipsoids at 50-percent probability. An asterisk indicates an equivalent atom that is related by symmetry.

TABLE XV.—SELECTED BOND LENGTHS AND BOND ANGLES WITH ESTIMATED STANDARD DEVIATIONS (NUMBERS IN PARENTHESES) FOR COMPOUNDS 3, 4, and 6 ($[Fe(NCS)_2(pic)_4]\cdot pic$, $[Co(NCS)_2(pic)_4]\cdot pic$, and $[Ni(NCS)_2(pic)_4]$, respectively)

Bond	Bond length, Å		
	M = Fe	M = Co	M = Ni
M–N1	2.105(7)	2.092(4)	2.073(3)
M–N2	2.231(6)	2.185(4)	2.131(3)
M–N2*	2.231(6)	2.187(4)	2.125(3)
M–N3	2.215(7)	2.178(4)	2.133(3)
M–N3*	2.215(7)	2.180(4)	2.127(3)
N1–C1	1.149(9)	1.140(6)	1.147(4)
C1–S1	1.617(9)	1.615(6)	1.625(4)
Bond	**Bond angle, deg**		
	M = Fe	M = Co	M = Ni
M–N1–C1	161.8(7)	155.1(4)	153.0(3)
N1–C1–S1	179.2(8)	179.4(4)	179.6(3)
N1–M–N1*	177.5(4)	177.3(2)	178.1(2)
N2–M–N3	177.3(2)	178.6(2)	178.6(1)
N1–M–N2	88.0(3)	90.2(2)	88.3(1)
N1–M–N3	89.3(3)	91.2(2)	90.4(1)
N1–M–N2*	90.2(3)	87.9(2)	90.4(1)
N1–M–N3*	92.5(3)	90.7(2)	91.0(1)
N2–M–N2*	89.6(3)	89.9(2)	89.6(1)
N2–M–N3*	90.4(2)	90.3(2)	90.9(1)

*Equivalent atom that is related by symmetry.

ring, which would average the methyl and nitrogen over all the sites. Solvent disorder in the Co-containing solid was even more pronounced. In compound 4, only a fraction of the guest solvent molecule could be located, and it too sat on a crystallographic $\bar{4}$ symmetry site, but at a different location than in compound 3. The disorder model consisted of two carbon atoms (C14 and C15), each with an occupancy of 0.25. The nickel compound was the same as desorbed β-$[Ni(NCS)_2(4\text{-mepy})_4]$, which was previously prepared by thermal decomposition of $[Ni(NCS)_2(4\text{-mepy})_4]\cdot C_6H_6$ followed by recrystallization in methanol (ref. 30).

Compounds 3, 4, and 6 have a distorted octahedral geometry, with two short axial M–NCS bonds (2.105(4), 2.092(4), and 2.073(3) Å for M = Fe, Co, and Ni, respectively) and four longer bonds to equatorial γ-picoline molecules (table XV). $M–N_{picoline}$ bond distances range from 2.215(7) to 2.231(6) Å for Fe, from 2.178(4) to 2.187(4) Å for Co, and from 2.125(3) to 2.133(3) Å for Ni. The observed decrease in M–N bond lengths in these structures from iron to nickel is consistent with the decrease in the atomic radii of the metals. The M–N=C bond angles for this series of compounds also decrease in magnitude from iron to nickel: 167.8(7)°, 155.1(4)°, and 153.0(3)° for the iron, cobalt, and nickel compounds, respectively. There has been controversy over the reason for, or significance of, the different M–N=C angles observed in clathrate structures with the same host but with different guest molecules. For at least compound 6 and $[Co(NCS)_2(pyr)_4]$ (where "pyr" = pyridine) it was determined that differences in M–N=C bond angles were simply a result of molecular packing in the solid rather than an electronic effect (refs. 29 and 33). All observed bond distances and angles in these structures are consistent with previously published structures (refs. 26, 30, 33, and 34). Approximate ring pitch angles for the attached γ-picoline molecules are 48° and 56° for the iron molecule, 50° and 58° for the cobalt molecule, and 50° and 56° for the nickel molecule. Dihedral angles of the bound solvent across the central metals are approximately 104.4°, 108.4°, and 105.7° for the iron, cobalt, and nickel molecules, respectively. These angles differ from other values reported for the same compounds with different guest molecules, but this simply demonstrates the ligand's ability to rotate around the metal-nitrogen σ-bond to accommodate guest molecules of various sizes and shapes (ref. 31).

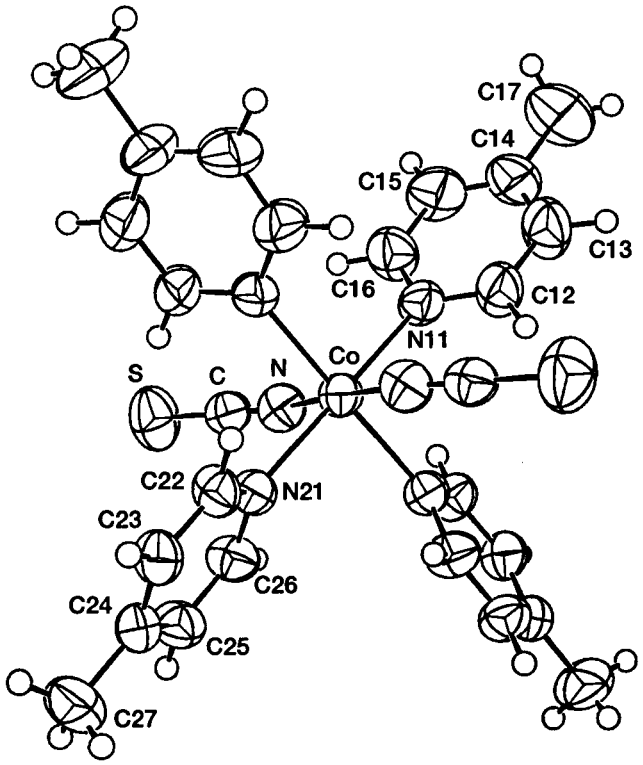

Figure 6.—ORTEP diagram of compound 5 ($Co(NCS)_2(pic)_4$) with hydrogens. Atoms are represented by ellipsoids at 50-percent probability.

TABLE XVI.—SELECTED BOND LENGTHS AND BOND ANGLES WITH ESTIMATED STANDARD DEVIATIONS (NUMBERS IN PARENTHESES) FOR COMPOUND 5 ($Co(NCS)_2(pic)_4$)

Bond	Bond length, Å	Bond	Bond angle, deg
Co–N	2.085(4)	Co–N–C	153.1(3)
Co–N11	2.167(3)	N–C–S	179.5(4)
Co–N21	2.169(3)	N–Co–N*	178.0(2)
N–C	1.150(5)	N11–Co–N21	178.3(1)
C–S	1.615(5)	N–Co–N11	90.5(1)
		N–Co–N21	87.9(1)
		N11–Co–N11*	88.4(2)

*Equivalent atom that is related by symmetry.

To help demonstrate that thiourea forms ammonium thiocyanate under reflux conditions, and that these materials could also be prepared using ammonium thiocyanate instead of thiourea, attempts were made to prepare compound 4 using ammonium thiocyanate. Single crystals grown from this reaction yielded compound 5, which did not contain occluded solvent, and afforded improved structural *R* values. Cobalt-nitrogen bond distances for compound 5 are consistently shorter than for the compound containing solvent (compound 4), but are within 3σ of each other, with $Co–N_{CS}$ bond lengths of 2.085(4) Å and $Co–N_{picoline}$ bond distance ranges of 2.167(3) to 2.169(9) Å (table XVI). Bond angles for the two cobalt-containing compounds are similarly within 3σ of each other. All other bond distances and angles are consistent with previously reported structures (refs. 33 to 35).

Reactions of thiourea with copper metal yielded three structures. One structure is molecular (compound 7), the second (compound 8) is best described as "pseudo-polymeric," since the molecules exhibit some long-range interactions, and the third is polymeric (compound 9). The preparation of each product depends on the stoichiometry of the starting materials and the reaction conditions, with each reaction giving good yield. Compound 7 (fig. 7) is a clathrate that was found with the guest sites 2/3 occupied by γ-picoline molecules and 1/3 occupied by water molecules. Since all solvents were dried and distilled prior to handling, and all manipulations were performed anaerobically under an argon atmosphere, the most plausible explanations for the occluded water are that the material was inadvertently exposed to air during crystal manipulation or that the Schlenkware leaked during crystal growth. Crystals of compound 7 were colorless while growing, but turned green when exposed to air during handling. It is likely that the color change coincides with the inclusion of the water.

Clathrates of $[Fe(NCS)_2(pic)_4]$ have been observed to vary in color with similar guest molecules. With derivatized benzene guest molecules, the color of the solid varies from light yellow (*m*-xylene clathrate) through light brown (benzene clathrate) to deep black (*p*-xylene clathrate) (ref. 26). In all three structures, the metrics of the iron molecules are nearly identical; the only structural difference is that the xylene clathrates contain some less than van der Waals distance interactions between the hydrogen atoms on the guest molecules and the sulfur atoms of the isothiocyanates. Before the cause of the color change in compound 7 can be determined, the structure of the colorless crystals will have to be determined; the results will be reported when available. The ability of clathrates to concentrate small concentrations of available water has been observed in $[Mn(NCS)_2(pic)_4]$ $\cdot 2/3pic \cdot 1/3H_2O$, $[Mg(NCS)_2(pic)_4] \cdot 2/3pic \cdot 1/3H_2O$, and $[Cd(NCS)_2(pic)_4] \cdot 2/3pic \cdot 1/3H_2O$ (refs. 25 and 36).

Compound 7 has a distorted octahedral geometry with two short $Cu–N_{sc}$ bonds of 1.981(4) Å, two short $Cu–N_{picoline}$ bonds of 2.051(4) Å, and two long $Cu–N_{picoline}$ bonds of 2.480(4) Å (table XVII). The short

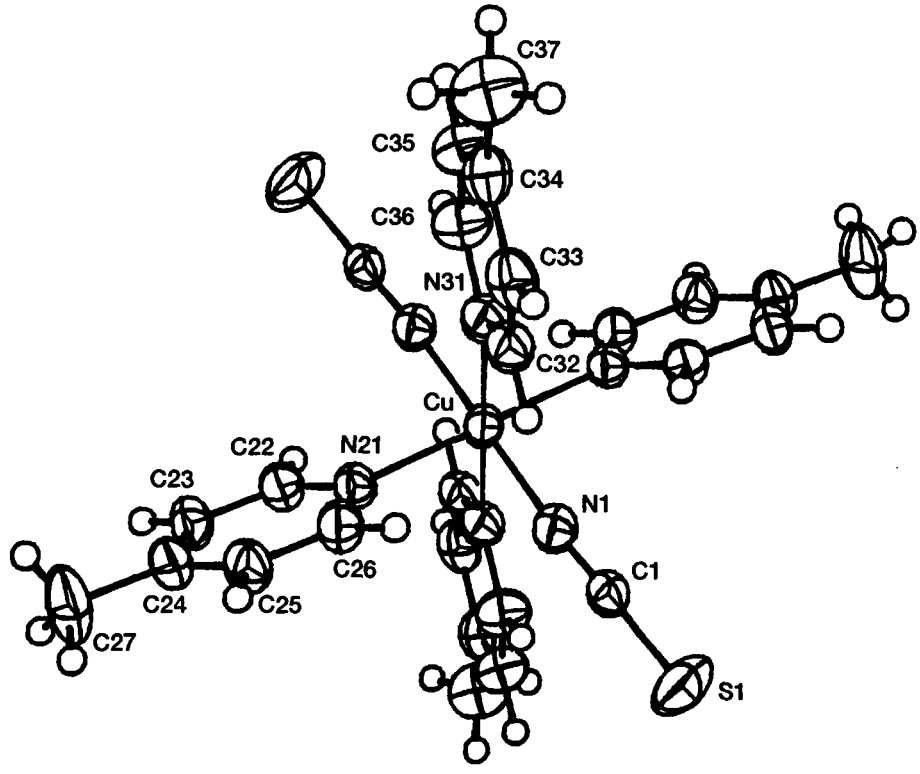

Figure 7.—ORTEP diagram of compound 7 ($Cu(NCS)_2(pic)_4$) with hydrogens. Atoms are represented by ellipsoids at 50-percent probability.

copper-picoline bonds of Cu–N21 are for picolines that interleave with other coordinated solvents, whereas the long copper-picoline bonds of Cu–N31 are for picolines that overlap with occluded solvent and H_2O. The nature of the difference in copper-picoline bond distances is unclear, but has previously been observed (ref. 25). All other bond distances and angles are consistent with previously published data (ref. 25).

Reactions with excess thiourea and copper metal yielded a five-coordinate copper(II) molecule. The unit cell for compound 8 consists of the copper-containing molecule $[Cu(NCS)_3(pic)_2]^-$, a protonated picoline molecule serving as the counterion, and a trapped 4-methylpyridine molecule. The Cu-containing molecule has a distorted square-pyramidal geometry, with the coordinated picoline and two isothiocyanates forming the basal plane and the remaining isothiocyanate bound at the apex (fig. 8). The compound has a layered structure with the copper atoms and isothiocyanate molecules lying in planes parallel to the (010) plane and located at $z = 0.25$ and 0.75. The coordinated picoline molecules extend above and below the copper-isothiocyanate layers and interleave with bound picoline from neighboring layers and occluded solvent molecules for efficient packing in the solid. $Cu–N_{picoline}$ bond distances are 2.039(7) Å and 2.050(7) Å (table XVIII). Two of the $Cu–N_{CS}$ bond distances are 1.928(9) Å and 1.968(9) Å, but the third is 2.23(1) Å. The elongated Cu–N7 bond is for the isothiocyanate molecule bound at the apical position, and it arises from long-range electronic interactions with neighboring Cu atoms. The apical isothiocyanate is positioned such that one of the lone pair of electrons on the

TABLE XVII.—SELECTED BOND LENGTHS AND BOND ANGLES WITH ESTIMATED STANDARD DEVIATIONS (NUMBERS IN PARENTHESES) FOR COMPOUND 7 ($[Cu(NCS)_2(pic)_4]\cdot 2/3pic\cdot 1/3H_2O$)

Bond	Bond length, Å	Bond	Bond angle, deg
Cu–N1	1.981(4)	Cu–N1–C1	159.7(4)
Cu–N21	2.051(4)	N1–C1–S1	177.8(5)
Cu–N31	2.480(4)	N1–Cu–N1*	180.0(0)
N1–C1	1.154(6)	N21–Co–N21*	180.0(0)
C1–S1	1.609(5)	N31–Cu–N31*	180.0(0)
		N1–Cu–N21	90.4(2)
		N1–Cu–N31	90.4(2)
		N21–Cu–N31	89.7(1)

*Equivalent atom that is related by symmetry.

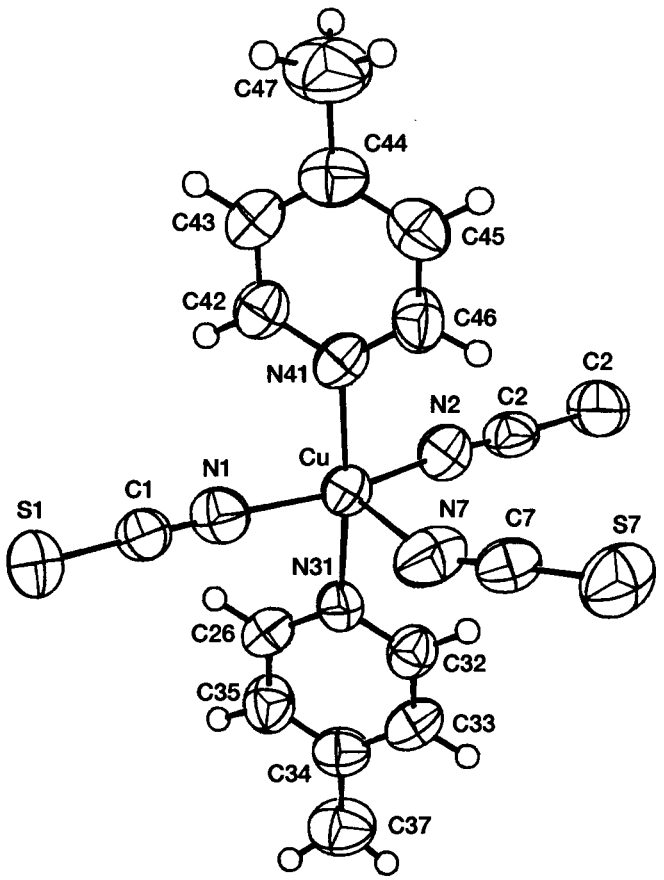

Figure 8.—ORTEP diagram of compound 8 ($[Cu(NCS)_3(pic)_2]^-$) with hydrogens. Atoms are represented by ellipsoids at 50-percent probability.

sulfur atom is directed toward the vacant site of the copper on a neighboring $[Cu(NCS)_3(pic)_2]^-$ molecule. The Cu–S7 distance for this interaction is 3.402(4) Å. Although this distance is outside the copper-sulfur van der Waals distance (3.25 Å), there undoubtedly are some long-range electrostatic interactions between the two atoms. This interaction allows the molecules to form one-dimensional "chains" that run perpendicular to the (101) plane. In addition, steric crowding limits the copper centers from moving closer together and allowing either the Cu–S or $Cu–N_{CS}$ bond to shorten.

Long Cu–S and elongated apical $Cu–N_{CN}$ bonds in pseudo five-coordinate copper-isothiocyanate compounds have been previously observed. In $[Cu(NCS)_2(3,4\text{-dimepy})_3]$ and $[Cu(NCS)_2(3\text{-mepy})_3]$ (ref. 37), the three substituted pyridine molecules and one of the isothiocyanate ligands form the basal plane of a distorted square-based pyramid, with the remaining isothiocyanate bound at the apex. In these molecules, the apical isothiocyanate bridges to another molecule at the vacant

TABLE XVIII.—SELECTED BOND LENGTHS AND BOND ANGLES WITH ESTIMATED STANDARD DEVIATIONS (NUMBERS IN PARENTHESES) FOR COMPOUND 8 ($(Hpic)[Cu(NCS)_3(pic)_2]\cdot pic$)

Bond	Bond length, Å	Bond	Bond angle, deg
Cu–N1	1.928(9)	Cu–N1–C1	175.0(8)
Cu–N2	1.968(9)	Cu–N2–C2	167.9(8)
Cu–N7	2.23(1)	Cu–N7–C7	149.4(9)
Cu–N31	2.050(7)	Cu–S7–C7	142.6(4)
Cu–N41	2.039(7)	N1–Cu–N2	165.4(4)
Cu–S7	3.402(4)	N7–Cu–S7	174.4(3)
N1–C1	1.15(1)	N7–Cu–N1	99.1(4)
N2–C2	1.15(1)	N7–Cu–N2	95.4(4)
N7–C7	1.17(1)	N7–Cu–N31	93.6(3)
C1–S1	1.60(1)	N7–Cu–N41	93.3(3)
C2–S2	1.61(1)	N1–Cu–N31	90.7(3)
C7–S7	1.59(1)	N1–Cu–N41	90.7(3)
		N1–Cu–S7	85.8(3)
		N2–Cu–N31	88.5(3)
		N2–Cu–N41	88.4(3)
		N2–Cu–S7	79.6(3)
		N31–Cu–S7	88.9(2)
		N41–Cu–S7	84.0(2)
		N1–C1–S1	179.0(1)
		N2–C2–S2	176.7(9)
		N7–C7–S7	179.4(9)

copper site through the sulfur with bond distances of 3.41(1) Å and 3.62(1) Å, respectively, for the two molecules. The apical Cu–N bonds for the two molecules are 2.22(2) Å and 2.219(1) Å, respectively. In the extended structure of [Cu(NCS)(cyclam)](SCN) (ref. 38), where cyclam is 1,4,8,11-tetraazacyclotetradecane, a similar apical $Cu–N_{CS}$ bond lengthening is observed. In the molecule, the cyclam forms the base of a square-based pyramid, with the isothiocyanate ligand at the apex. Again the thiocyanate molecule bridges to a neighboring molecule at the vacant copper site, giving $Cu–N_{CS}$ and Cu–S bond distances of 2.430(4) Å and 3.015(1) Å, respectively.

All three isothiocyanate groups in $[Cu(NCS)_3(pic)_2]^-$ are nearly linear, with the N=C=S bond angle ranging from 176.7(9)° to 179.4(9)°. The Cu–N=C bond angles are 167.9(9)° and 175.0(8)° for the terminal isothiocyanates and 149.4(9)° for the bridging isothiocyanate. The Cu–S=C bond angle for the bridging isothiocyanate is 142.6(4)°. In the $[Cu(NCS)_3(pic)_2]^-$ chains, the planes formed by the $Cu(NCS)_3$ units rock back and forth around the chain axis with a dihedral angle between alternating planes of approximately 30°. All other bond distances and angles are as expected and compare well with other copper-isothiocyanate-substituted pyridine compounds.

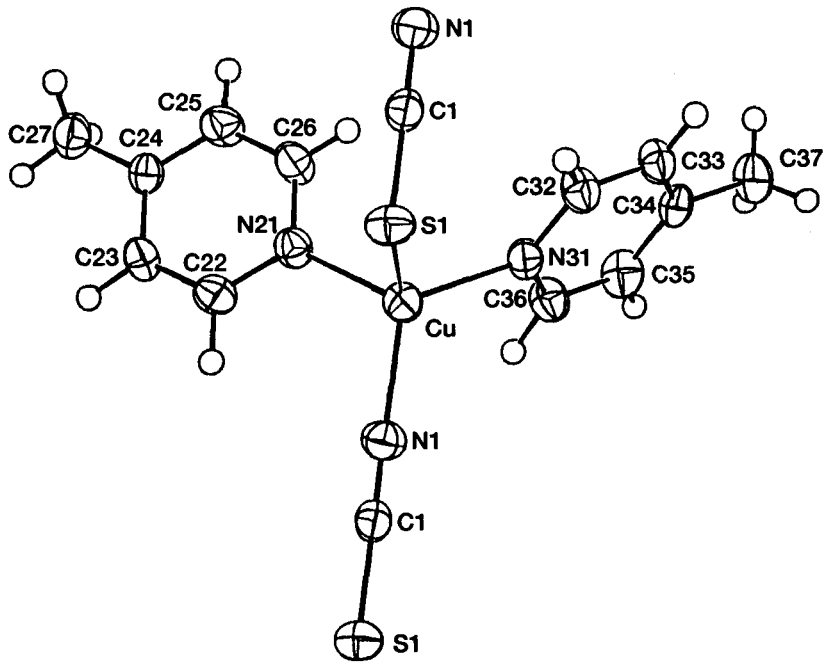

Figure 9.—ORTEP diagram of compound 9 ($[Cu(NCS)(pic)_2]_n$) with hydrogens. Atoms are represented by ellipsoids at 50-percent probability.

The final material, compound 9, is a polymeric structure and is the only copper(I) compound that was isolated. It is a one-dimensional structure with thiocyanate groups linking $[Cu(pic)_2]^+$ units to form chains that run perpendicular to the (010) plane (fig. 9). The unit cell contains two chains, which are related by a two-fold screw axis. The four-coordinate copper(I) has a distorted tetrahedral geometry. Copper bond distances to the bridging thiocyanate molecule are 1.945(3) Å and 2.3562(9) Å for $Cu–N_{CS}$ and $Cu–S_{CN}$, respectively (table XIX). $Cu–N_{picoline}$ bond distances are 2.061(2) Å and 2.068(3) Å. Significant bond angles are 111.44(9)° for N1–Cu–S1, 108.9(1)° for N21–Cu–N31, 170.9(3)° for Cu–N1–C1, and 100.3(1)° for Cu–S1–C1. All other thiocyanate and solvent molecule bond lengths and angles are as expected. These bond distances and angles are comparable to those reported by Healy et al. for the same compound prepared by recrystallizing copper(I) thiocyanate from 4-methylpyridine (ref. 39).

Traditionally, thiocyanate and isothiocyanate compounds have been prepared in solution by reacting metal salts with thiocyanate salts and donor ligands or from $M(SCN)_n$ and donor ligands. However, the products reported here were prepared by refluxing metal powders with excess thiourea in 4-methylpyridine. Several early reactions were attempted using pyridine, but no crystalline products were formed. The reactions appear to be quantitative, and in a few cases after crystallization, what remains is a flask full of crystals and a nearly colorless solution.

Although the reactions are a "one-pot synthesis," the mechanism for the reaction is not completely understood. It is well documented that thiourea can be prepared from solutions of NH_4SCN, with reported yields ranging from 25 to 95 percent (refs. 40 and 41) and that the equilibrium concentration ratio of NH_4SCN to thiourea (NH_4SCN:$S=C(NH_2)_2$) is approximately 0.75:0.25 in propanol and butanol at temperatures near the boiling point of 4-methylpyridine (145 °C) (ref. 42). Therefore, the most probable pathway for the reactions is that,

TABLE XIX.—SELECTED BOND LENGTHS AND BOND ANGLES WITH ESTIMATED STANDARD DEVIATIONS (NUMBERS IN PARENTHESES) FOR COMPOUND 9 ($[Cu(NCS)(pic)_2]_n$)

Bond	Bond length, Å	Bond	Bond angle, deg
Cu–N1	1.945(3)	N1–Cu–S1	111.44(9)
Cu–S1	2.3562(9)	N1–Cu–N21	108.2(1)
Cu–N21	2.068(3)	N1–Cu–N31	115.3(1)
Cu–N31	2.061(2)	S1–Cu–N21	103.72(8)
N1–C1	1.159(5)	S1–Cu–N31	108.63(8)
C1–S1	1.641(4)	N21–Cu–N31	108.9(1)
		Cu–N1–C1	170.9(3)
		Cu–S1–C1	100.3(1)
		N1–C1–S1	177.7(3)

under picoline reflux conditions, a portion of the thiourea is converted to the salt and the metal reacts with the thiocyanate ions present in solution and forces the isomerization reaction (eq. (1)) to the right.

$$S{=}C(NH_2)_2 \rightleftharpoons SCN^- + NH_4^+ \qquad (1)$$

In the case of compound 7, where the solution was only heated to 75 °C, the copper likely scavenges what little thiocyanate is in solution and again pulls the reaction to the right. However, this pathway fails to account for the observed oxidation of the metals during the reaction. A potential source of metal oxidation is impurities in the solvent, but all solvents were rigorously dried and distilled under nitrogen prior to use. Another possibility is contamination of the metal powders with metal oxide impurities; the isolated products are simply the result of the oxidized metal reacting with the isothiocyanate ions in solution and leaving the unoxidized metal unreacted. This scenario also seems unlikely given the metal powders were completely consumed during almost all the reactions. One last possibility to consider is the reduction of NH_4^+ or protonated γ-picoline at the reflux temperatures of 4-methylpyridine to yield NH_3 and H_2 or γ-picoline and H_2, which would require one electron per NH_4^+ or $Hpic^+$ that is reduced. Some empirical evidence does support the hypothesis; during the early stages of many of the reactions, gas evolution was observed. However, no attempt was made to isolate or characterize the gas. Any NH_3 or H_2 formed during the reaction would out-gas from the solution during reflux conditions and, thus, pull the reaction to the right. Furthermore, with the exception of copper, all metals that have yielded crystalline products have a negative aqueous standard reduction potential in comparison to the reduction potential of hydrogen (0.0 V, E°) (ref. 43).

It is also unknown how general the reaction is. In addition to Mn, Fe, Co, Ni, and Cu, this synthetic protocol was attempted using In, Ti, V, Cr, and Zr, but (with the exception of Cr) these reactions have yet to yield crystalline material. Small crystals were obtained from reactions with Cr powder, but the crystals were of insufficient size for single-crystal x-ray crystallography.

In summary, the synthetic pathway is not yet fully understood, but it has yielded three new compounds and offers an alternative route to previously reported materials. The synthetic mechanism and the oxidation of the metal powders are currently under investigation, and the results will be reported in a future communication.

Conclusions

During our effort to prepare new single-source precursor molecules that could be used to deposit device-quality material at low temperatures, a general synthetic route to metal-isothiocyanate materials was discovered, and three new anionic metal-isothiocyanate-4-methylpyridine complexes were synthesized and structurally characterized.

Rather than using a thiocyanate salt as the source for the isothiocyanate, thiourea served as the anion source. Thiourea was converted to ammonium thiocyanate in solution during reflux in 4-methylpyridine and then reacted with metal powders to form a series of metal coordination compounds of the type $[M(NCS)_x(pic)_y]$. It is not known how general the reaction is in preparing metal-isothiocyanate materials. Reactions with iron and copper yielded multiple products, with the composition of each product dependent on the stoichiometry of the reactants.

Supplementary Materials Available

A complete listing of anisotropic displacement parameters, interatomic distances, angles, hydrogen coordinates, displacement parameters, and structure factor amplitudes for the reported compounds are available upon request from the authors. Atomic coordinates for the structural analyses have been deposited with the Cambridge Crystallographic Data Center.

National Aeronautics and Space Administration
John H. Glenn Research Center at Lewis Field
Cleveland, Ohio 44135, August 19, 2002

Appendix—Symbols

a	length of the a axis or unit cell edge
b	length of the b axis or unit cell edge
c	length of the c axis or unit cell edge
Cc	space group number 9
CCDC	Cambridge Crystal Data Center
GOF	goodness of fit
$I \geq 3\sigma(I)$	number of reflections with intensity greater than or equal to three times the standard deviation
$I4_1/a$	space group number 88
$P2_1$	space group number 4
$P2_1/n$	space group number 14
R	$\Sigma \lvert F_o - F_c \rvert / \Sigma \lvert F_o \rvert$
R_w	$\left[\Sigma\, w(F_o - F_c)^2 / \Sigma\, w F_o^{\,2}\right]^{0.5}$
$R\bar{3}$	space group number 148
V	volume of the unit cell
Z	number of repeating formula units per unit cell
α	angle between the b and c edges of the unit cell
β	angle between the a and c edges of the unit cell
γ	angle between the a and b edges of the unit cell
μ	linear absorption coefficient
$\omega - 2\theta$	scan technique that was used to collect the x-ray data
$2\theta_{max}$	maximum angle in the 2θ direction to which data were collected

References

1. Flood, Dennis J.: Thin Film Photovoltaics—Status and Applications to Space Power. Proceedings of the 34th National Heat Transfer Conference, NHTC2000–12068, Pittsburgh, Aug. 20–22, PA, 2000.
2. Raffaelle, R.P., et al.: Electrochemical Synthesis of $CuInSe_2$ for Thin Film Devices. Materials Science in Semiconductor Processing, vol. 2, 1999, pp. 289–296.
3. Raffaelle, R.P., et al.: Electrodeposited $CuInSe_2$ Thin Film Junctions. NASA/TM—1997-206322, 1997. http://gltrs.grc.nasa.gov/cgi-bin/GLTRS/browse.pl?1997/TM-97-206322.html Accessed October 23, 2002.
4. Raffaelle, R.P., et al.: A Facile Route to Thin-Film Solid State Lithium Microelectronic Batteries. J. Power Sources, vol. 89, 2000, pp. 52–55.
5. Rockett, A.; and Birkmire, R.W.: $CuInSe_2$ for Photovoltaic Applications. J. Appl. Phys., vol. 70, no. 7, 1991, pp. R81–R97.
6. Jones, Steven D.; and Akridge, James R.: A Microfabricated Solid-State Secondary Li Battery. SSIOD, vols. 86–88, pt. II, 1996, pp. 1291–1294.
7. Jones, Steven D.; and Akridge, James R.: Development and Performance of a Rechargeable Thin-Film Solid-State Microbattery. J. Power Sources, vol. 54, no. 1, 1995, pp. 63–67.
8. Wang, B., et al.: Characterization of Thin-Film Rechargeable Lithium Batteries with Lithium Cobalt Oxide Cathodes. J. Electrochem. Soc., vol. 143, no. 10, 1996, pp. 3203–3213.
9. Banger, K.K., et al.: Facile Modulation of Single Source Precursors: The Synthesis and Characterization of Single Source Precursors for Deposition of Ternary Chalcopyrite Materials. Thin Sol. Fi., vols. 403–404, 2002, pp. 390–395.
10. Kankam, M. David, et al.: Recent GRC Aerospace Technologies Applicable to Terrestrial Energy Systems. AIAA Paper AIAA–2000–2955, 2000.
11. Zhou, X., et al.: Synthesis and Structural Characterization of Bis (4-methylpyridine)Dichloro (dimethyldithiocarbamate) gallium(III), $GaC_{12}(4\text{-mepy})_2(S_2CN(CH_3)_2)$. Main Group Metal Chemistry, vol. 22, no. 1, 1999, pp. 35–39.
12. Macinnes, Andrew N., et al.: Enhancement of Photoluminescence Intensity of GaAs With Cubic GaS Chemical Vapor Deposited Using a Structurally Designed Single-Source Precursor. Appl. Phys. Lett., vol. 62, no. 7, 1993, pp. 711–713.
13. Tabib-Azar, Massood, et al.: Electronic Passivation of n- and p-type GaAs Using Chemical Vapor Deposited GaS. Appl. Phys. Lett., vol. 63, no. 5, 1993, pp. 625–627.
14. Harris, J.D., et al.: Atmospheric Pressure Spray Chemical Vapor Deposited $CuInS_2$ Thin Films for Photovoltaic Applications. 17th Space Photovoltaic Research and Technology Conference. NASA/CP—2002-211831, 2002, pp. 84–90.
15. Harris, J.D., et al.: Using Single Source Precursors and Spray Chemical Vapor Deposition to Grow Thin-Film $CuIns_2$. Conference Record of the Twenty-Eighth IEEE Photovoltaic Specialists Conference, IEEE, New York, NY, 2000, pp. 563–566.
16. Hollingsworth, J.A.; Hepp, A.F.; and Buhro, W.E.: Spray CVD of Copper Indium Disulfide Films: Control of Microstructure and Crystallographic Orientation. Chemical Vapor Deposition, vol. 5, no. 3, 1999, pp. 105–108.
17. Hollingsworth, J.A., et al.: Spray Chemical Vapor Deposition of $CuInS_2$ Thin Films for Application in Solar Cell Devices. Mat. Res. Soc. Symp. Proc., vol. 495, 1998, pp. 171–176.
18. Henderson, D.O., et al.: Optical and Structural Characterization of Copper Indium Disulfide Thin Films. Mater. Design, vol. 22, no. 7, 2001, pp. 585–589.
19. Banger, K.K.; Cowen, J.; and Hepp, A.F.: Synthesis and Characterization of the First Liquid Single-Source Precursors for the Deposition of Ternary Chalcopyrite ($CuInS_2$) Thin Film Materials. Chemistry of Materials, vol. 13, no. 11, 2001, p. 3827.
20. Frost, Jack G.: Oxidative Destruction of Thiourea in Boiler Chemical Cleaning Waste Solutions. Environ. Sci. Technol., vol. 27, no. 9, 1993, pp. 1871–1874.
21. Walker, N.; and Stuart, D.: An Empirical-Method for Correcting Diffractometer Data for Absorption Effects. Acta Crystallogr. A, vol. 39, 1983, pp. 158–166.
22. Sheldrick, G.: SHELXS–86. Program for Crystal Structure Solution, University of Göttingen, Göttingen, Germany, 1986.
23. Fair, C.K.: MoleN. An Interactive Intelligent System for Crystal Structure Analysis, Enraf-Nonius, Delft, The Netherlands, 1990.
24. teXsan for Windows. Structural Analysis Package, Molecular Structure Corporation, Woodlands, TX, 1992.
25. Pervukhina, N.V., et al.: Peculiarities of the Crystal-Structure and Packing of the Host and Guest Molecules in the $[M(4\text{-MePy})_4(NCS)_2]\cdot 0.67(4\text{-MePy})\cdot 0.33\ H_2O$ Clathrates (M = Cu(II), Mn(II); 4-MePy = 4-Methylpyridine). J. Inclusion Phenom. Mol. Recognit. Chem., vol. 13, no. 1, 1992, pp. 9–16.
26. Lipkowski, Janusz: Crystal Structures of the Clathrate Inclusion Compounds Formed by the Host Bis(Isothiocyanato) tetrakis (4-methylpyridine) iron(II) with Benzene, *m*-Xylene and *p*-Xylene as Guests. J. Inclusion Phenom. Mol. Recognit. Chem., vol. 8, no. 4, 1990, pp. 439–448.
27. Harris, J.D., et al.: Room Temperature Dissolution of Metal Powders by Thiourea: A Novel Route to Transition Metal Isothiocyanate Complexes. Mater. Des., vol. 22, no. 7, 2001, pp. 625–634.
28. Schaeffer, William D., et al.: Separation of Xylenes, Cymenes, Methylnaphthalenes and Other Isomers by Clathration with Inorganic Complexes. J. Am. Chem. Soc., vol. 79, no. 22, 1957, pp. 5870–5876.
29. Lipkowski, Janusz; Sgarabotto, Paolo; and Andreetti, Giovanni D.: Clathrate Inclusion Compounds of Bis(isothiocyanato)tetrakis (4-methylpyridine)-nickel(II). Part III. Bis(isothiocyanato)tetrakis (4-methylpyridine)nickel(II)-1-Methylnapthalene (1:2). Acta Crystallogr. B, vol. 38, 1982, pp. 416–421.
30. Andreetti, G.D.; Bocelli, G.; and Sgarabotto, P.: Bis(Isothiocyanato) tetrakis (4-methylpyridine)nickel(II) $C_{26}H_{28}N_6NiS_2$. Cryst. Struct. Comm., vol. 1, 1972, pp. 51–54.
31. Bond, Dianne R.; Jackson, Graham E.; and Nassimbeni, Luigi R.: Studies in Werner Clathrates. Part I. Structures of Bis(Isocyanato) bis(4-methylpyridine) Bis (4-phenylpyridine)nickel(II)•Methyl Cellosolve and Bis (Isothiocyanato)tetra(4-methylpyridine)-nickel(II)•*p*-cymene. S. Afr. J. Chem., vol. 36, no. 1, 1983, pp. 7–9.
32. Allison, S.A.; and Barrer, R.M.: Sorption in the β-Phases of Transition Metal(II) Tetra-(4-methylpyridine) Thiocyanates and Related Compounds. J. Chem. Soc. (A), 1969, pp. 1717–1723.

33. Hartl, Hans; and Brüdgam, Irene: *trans*-Bis(isothiocyanato) tetrakis(pyridin)kobalt(II). Acta Crystallogr. B, vol. 36, 1980, pp. 162–165.
34. Foxman, Bruce M.; and Mazurek, Harry: The Structure and Solid-State Reactivity of a New Polymorph of Tetrakis(4-vinylpyridine)diisothiocyanatocobalt(II). Inorganica Chimica Acta, vol. 59, no. 2, 1982, pp. 231–235.
35. Belitskus, D., et al.: Single Crystal Studies on Some Clathrates of Tetra-(4-methylpyridine)-nickel(II) and Cobalt Dithiocyanates. Inorg. Chem., vol. 2, no. 4, 1963, pp. 873–875.
36. Lipkowski, J.; and Soldatov, D.V.: Two Clathrates of Bis(Isothiocyanato)tetrakis(4-methylpyridine)magnesium(II) as a Host with 4-Methylpyridine as a Guest. J. Inclusion Phenom. Mol. Recognit. Chem., vol. 18, no. 4, 1994, pp. 317–329.
37. Kabešová, Mária; and Kožišková, Zlatica: The Crystal and Molecular Structure of Thiocyanato-Copper(II) Complexes With 3-Methylpyridine and 3,4-Dimethylpyridine. Collec. Czechosl. Chem. Commun., vol. 54, no. 7, 1989, pp. 1800–1807.
38. Lu, Tian-Huey, et al.: (Isothiocyanato)[1*RS*,4*RS*,8*SR*,11*SR*)-1,4,8,11-tetraazacyclotetradecane]copper(II) Thiocyanate, [Cu(NCS)(cyclam)](SCN). Acta Crystallogr., vol. C52, pt. 5, 1996, pp. 1093–1095.
39. Healy, Peter C., et al.: Lewis Base Adducts of Group 1B Metal(I) Compounds. 9. Synthesis and Crystal Structures of Adducts of Copper(I) Thiocyanate with Substituted Pyridine Bases. Inorg. Chem., vol. 23, no. 23, 1984, pp. 3769–3776.
40. Powers, Robert E.; and Mitchell, John: Preparation of Thiourea, U.S. Patent 2,560,596, 1951.
41. Arnikar, H.J., et al.: Radiation-Induced Isomerization of Thiourea Into Ammonium Thiocyanate. J. Radioanal. Nucl. Chem., vol. 185, no. 2, 1994, pp. 227–230.
42. Burrows, G.H.: The Equilibrium Between Thio-Urea and Ammonium Thiocyanate. J. Am. Chem. Soc., vol. 46, 1924, pp. 1623–1627.
43. Weast, Robert C.; Astle, Melvin J.; and Beyer, William H., eds.: CRC Handbook of Chemistry and Physics: A Ready-Reference Book of Chemical and Physical Data. CRC Press, Boca Raton, FL, 1986.

REPORT DOCUMENTATION PAGE

Form Approved
OMB No. 0704-0188

1. AGENCY USE ONLY (*Leave blank*)	2. REPORT DATE	3. REPORT TYPE AND DATES COVERED
	July 2003	Technical Paper

4. TITLE AND SUBTITLE

Novel Route to Transition Metal Isothiocyanate Complexes Using Metal Powders and Thiourea

5. FUNDING NUMBERS

WU–755–A4–01–00

6. AUTHOR(S)

Jerry D. Harris, William E. Eckles, Aloysius F. Hepp, Stan A. Duraj, David G. Hehemann, Phillip E. Fanwick, and John Richardson

7. PERFORMING ORGANIZATION NAME(S) AND ADDRESS(ES)

National Aeronautics and Space Administration
John H. Glenn Research Center at Lewis Field
Cleveland, Ohio 44135–3191

8. PERFORMING ORGANIZATION REPORT NUMBER

E–13573

9. SPONSORING/MONITORING AGENCY NAME(S) AND ADDRESS(ES)

National Aeronautics and Space Administration
Washington, DC 20546–0001

10. SPONSORING/MONITORING AGENCY REPORT NUMBER

NASA TP—2003-211890

11. SUPPLEMENTARY NOTES

Jerry D. Harris, Cleveland State University, Cleveland, Ohio 44115, and NASA Resident Research Associate at Glenn Research Center; William E. Eckles, Stan A. Duraj, and David G. Hehemann, Cleveland State University, Cleveland, Ohio 44115; Aloysius F. Hepp, NASA Glenn Research Center; Phillip E. Fanwick, Purdue University, West Lafayette, Indiana 47907; and John Richardson, University of Louisville, Louisville, Kentucky 40292. Responsible person, Aloysius F. Hepp, organization code 5410, 216–433–3835.

12a. DISTRIBUTION/AVAILABILITY STATEMENT

Unclassified - Unlimited
Subject Category: 25 Distribution: Standard

Available electronically at http://gltrs.grc.nasa.gov

This publication is available from the NASA Center for AeroSpace Information, 301–621–0390.

12b. DISTRIBUTION CODE

13. ABSTRACT ***(Maximum 200 words)***

A new synthetic route to isothiocyanate-containing materials is presented. Eight isothiocyanate-4-methylpyridine (γ-picoline) compounds were prepared by refluxing metal powders (Mn, Fe, Co, Ni, and Cu) with thiourea in γ-picoline: compound 1—$(Hpic)_2[Mn(NCS)_4(pic)_2]\cdot 2pic$, compound 2—$(Hpic)_2[Fe(NCS)_4(pic)_2]\cdot 2pic$, compound 3—$[Fe(NCS)_2(pic)_4]\cdot pic$, compound 4—$[Co(NCS)_2(pic)_4]\cdot pic$, compound 6—$[Ni(NCS)_2(pic)_4]$, compound 7—$[Cu(NCS)_2(pic)_4]\cdot 2/3pic\cdot 1/3H_2O$, compound 8—$(Hpic)[Cu(NCS)_3(pic)_2]\cdot pic$, and compound 9—$[Cu(NCS)(pic)_2]_x$ (where pic = γ-picoline). Compound 5—$[Co(NCS)_2(pic)_4]$—was prepared by refluxing the metal powder with ammonium thiocyanate in γ-picoline. With the exception of compound 5, the isothiocyanate ligand was generated in situ by the isomerization of thiourea to $NH_4^+SCN^-$ at reflux temperatures. The complexes were characterized by x-ray crystallography. Compounds 1, 2, and 8 are the first isothiocyanate-4-methylpyridine anionic compounds ever prepared and structurally characterized. Compounds 1 and 2 are isostructural with four equatorially bound isothiocyanate ligands and two axially bound γ-picoline molecules. Compound 8 is a five-coordinate copper(II) molecule with a distorted square-pyramidal geometry. Coordinated picoline and two isothiocyanates form the basal plane and the remaining isothiocyanate is bound at the apex. Structural data are presented for all compounds.

14. SUBJECT TERMS

Thiocyanate; Isothiocyanate; Methylpyridine; Picoline; Crystal structure; Inorganic chemistry; Synthesis (chemistry); Coordination; Solar cells

15. NUMBER OF PAGES

28

16. PRICE CODE

17. SECURITY CLASSIFICATION OF REPORT	18. SECURITY CLASSIFICATION OF THIS PAGE	19. SECURITY CLASSIFICATION OF ABSTRACT	20. LIMITATION OF ABSTRACT
Unclassified	Unclassified	Unclassified	